Smart Structures and Systems, *Vol. 26*, *No. 6* (*2020*) *781-796*
DOI: https://doi.org/10.12989/sss.2020.26.6.781

Prediction of total sediment load: A case study of Wadi Arbaat in eastern Sudan

Ali Aldrees [1], Abubakr Taha Bakheit [1,2] and Hamid Assilzadeh*[3]

[1] *Department of Civil Engineering, College of Engineering, Prince Sattam bin Abdulaziz University, Al-kharj 11942, Saudi Arabia*
[2] *Department of Civil Engineering, Faculty of Engineering, Red Sea University, Port Sudan, Sudan*
[3] *Institute of Research and Development, Duy Tan University, Da Nang 550000, Vietnam*

(*Received May 9, 2020, Revised November 15, 2020, Accepted November 21, 2020*)

Abstract. Prediction of total sediment load is essential in an extensive range of problems such as the design of the dead volume of dams, design of stable channels, sediment transport in the rivers, calculation of bridge piers degradation, prediction of sand and gravel mining effects on river-bed equilibrium, determination of the environmental impacts and dredging necessities. This paper is aimed to investigate and predict the total sediment load of the Wadi Arbaat in Eastern Sudan. The study was estimated the sediment load by separate total sediment load into bedload and Suspended Load (SL), independently. Although the sediment records are not sufficient to construct the discharge-sediment yield relationship and Sediment Rating Curve (SRC), the total sediment loads were predicted based on the discharge and Suspended Sediment Concentration (SSC). The turbidity data NTU in water quality has been used for prediction of the SSC in the estimation of suspended Sediment Yield (SY) transport of Wadi Arbaat. The sediment curves can be used for the estimation of the suspended SYs from the watershed area. The amount of information available for Khor Arbaat case study on sediment is poor data. However, the total sediment load is essential for the optimal control of the sediment transport on Khor Arbaat sediment and the protection of the dams on the upper gate area. The results show that the proposed model is found to be considered adequate to predict the total sediment load.

Keywords: total sediment load; prediction; bed load; suspended load; Khor Arbaat; annual runoff

1. Introduction

The sediment that is constantly supplied and hydraulically carried in channels and streams is provided by rainfall, runoff and river channel erosion. All reservoirs established by constructing dams on natural rivers are subjected to some degree of deposition and Sediment Inflow (SI) (Morris and Fan 1997). Due to the very low velocity in reservoirs, they have a tendency to be very effective sediment traps. Hence, during the life of the dam, the amount of reservoir sedimentation should be predicted. If the SI is large concerning the capacity of reservoir storage, the effective life of the reservoir may be short. For instance, a small reservoir (upper gate dam) on the Khor Arbaat near Port Sudan city was filled with sediment during the first years of operation. Different prediction techniques have been introduced for estimation and optimization applications. Prediction quality depends on a variety of variables such as error, soft computing approach and available problems. Artificial Intelligence (AI) methods are proposed to alleviate estimation problems. By interlacing with classical optimization algorithms, AI techniques have become essential prediction ways. Classical optimization procedures such as ant colony, bee colony, particle swarm, and firefly algorithms are used to address some shortcomings in the way of prediction. The neural network is also employed with AI techniques to enhance the efficiency of the prediction, while the hybrid algorithms were proposed for different types of objective evaluations. Machine learning and deep learning are other types of AI techniques, which are used and developed during estimation purposes. Employing these techniques for prediction, describing runoff volume, debris volume and sediment texture as input instead of output can lead to predicting the different loads (Shariati *et al*. 2019a, c, d, e, 2020b, c, d, Mohammadhassani *et al*. 2013, 2014, 2015, Toghroli *et al*. 2014, 2016, 2018, Toghroli 2015, Safa *et al*. 2016, 2020, Sadeghipour Chahnasir *et al*. 2018, Sedghi *et al*. 2018, Katebi *et al*. 2019, Mansouri *et al*. 2019, Trung *et al*. 2019, Zhao *et al*. 2019, 2020a, Alabduljabbar *et al*. 2020, Alaskar *et al*. 2020, Alyousef *et al*. 2020, Armaghani *et al*. 2020, Cao *et al*. 2020a, b, c, Liu *et al*. 2020, Qi 2020) no matter what kind of loads will be applied. Between the most important leads related to structures, those related to dynamic response of structures are on top (Moghaddam *et al*. 2009, Arabnejad Khanouki *et al*. 2010, Fanaie *et al*. 2012, 2014, 2015a, b, 2016a, b, Jalali *et al*. 2012, Shariati *et al*. 2012a, b, 2013, 2017, 2018, 2019a, 2020g, Khorami *et al*. 2017a, b, Zandi *et al*. 2018, Milovancevic *et al*. 2019, Shariati 2020) and those related to dam like sediment load. Sediment ingredients may consist of different debris such as crushed rocks, sand, marble and other types of probable waste sludge. The mechanical properties of the sediment may be similar to that of specific soils in which most parts

*Corresponding author, Ph.D.,
E-mail: abtaba@outlook.com

ISSN: 1738-1584 (Print), 1738-1991 (Online)

of them are sediment. Hence using previous studies data about mechanical properties of muddy soils could be helpful (Afrazi *et al*. 2018, 2019, Safa *et al*. 2019, Shariati *et al*. 2019a, 2020a, f, Suhatril *et al*. 2019, Majedi *et al*. 2020a, b, Rouhanifar *et al*. 2020, Yazdani *et al*. 2020, Zhao *et al*. 2020b).

The infilling process of river sand mining was investigated experimentally as well as using the CCHE2D numerical model. The result indicated that the numerical model overestimates the bedload transport in the degraded channel (Haghnazar *et al*. 2020). Suspended and bed load transport are two types of sediment transport in watersheds. The particles that are kept suspended by vertical part of velocity in turbulent flux are called suspended sediments. Moreover, the suspended sediment transport is mainly controlled by the velocity of flow, while the coarsest sediments might have only occasionally movement (Edwards *et al*. 1999, Okcu *et al*. 2016). Unlike suspended sediment that moves mainly in suspension, the bed load moves close to the streambed. It is normal to see moving, rolling and sliding of these particles in contact with streambed, while the third sort of motion is recognized as saltation. However, high-intensity flows lead to keeping the bedload immediately in suspension (Frey 2014), usually varying from 5 to 25% of suspended sediment transport (Yang 1996, Doğan *et al*. 2007). Two methods are available in order to obtain the values defining sediment loads in streams. One is based on direct measurement of the quantities of interest, and the other on relations developed between hydraulic parameters and sediment transport potential. In the following parts, the most common methods for both methods are shortly discussed.

Also, the movement of coarser sediments is managed by selective transport capacity, which shows the concentration of various sizes of sediments in the cross-section. Through the world, the need for improved understanding the physics of sediment transport is presently considered as one of the most important topics that have been highlighted in sedimentation with dams, particularly, nearly, more than half the reservoirs of the world which face problems of siltation (McCully 1996). In recent decades, river engineers have faced a number of challenges, the most important of which is the estimation of sediment load. Two methods are typically applied: 1) Total sediment load is directly calculated from the measured flow and sediment properties; 2) total sediment load is separated into bedload and SL which are estimated independently. Practical engineers prefer to employ the total load equation for determining sediment load since the criteria that separate bedload and SL is still a controversial topic (Duan 2013).

However, SL is a material, which moves in suspension and sustained in the water column by turbulence or in colloidal suspension or the material collected in or measured from a Suspended Sediment Load (SSL) sampler. As shown in Fig. 1, the total sediment load is defined by three ways of wash load, bed material load, and SL, as stated by Morris and Fan (1997). Moreover, due to of runoff from precipitation (rainfall or snowmelt), soil particles on the surface of a catchment, watershed and basin can be eroded and carried through the processes of the sheet, scald,

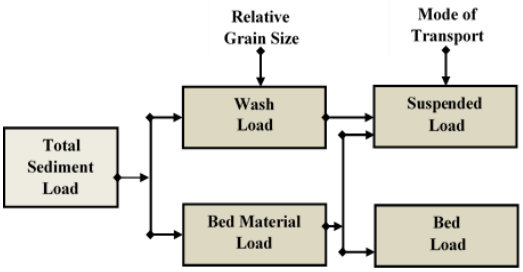

Fig. 1 Classification of sediment transport by grain size relative to the streambed and by mode of transport (source: Morris and Fan (1997))

rill and gully erosion. During erosion, sediment particles are carried through a stream system and are finally deposited in the dam's reservoirs or at the sea coast. According to Strand and Pemberton (1987) and Morris and Fan (1997), the following factors can determine a watershed's SY, which is (i) rainfall amount, intensity and runoff, (ii) soil type, geologic formation, ground cover and land use, (iii) topography, (iv) upland erosion rate, drainage network density, slope, shape, size and alignment of channels, (v) sediment characteristics-grain size, mineralogy and (vi) channel hydraulic characteristics.

With the passage of time, the sediment amount exported by a watershed basin shows the SY. It also indicates the amount, which will enter a reservoir placed at the downstream limit of its tributary watershed. The yield per unit of land area is known as the specific SY. The SY correlation to erosion is complicated by the issue of determining the sediment delivery ratio, which leads to the difficulty in estimation of the sediment load that was entering a reservoir based on the erosion rate within the watershed (Morris and Fan 1997). In order to size the Sediment Storage Pool (SSP) and evaluate life of reservoir, the estimations of long-term SY have been employed for several decades. However, these estimations are mostly incorrect, and sediments are accumulated by many reservoirs more quickly than initially planned. During relatively short times of flood discharges, most sediment is exported from watersheds. These incidents should be carefully managed in order to supply information on the long-term yield in addition to the time-wise change in load required to assess sediment routing strategies (Morris and Fan 1997).

If the proportion of particles of different sizes remains constant in the flow, turbidity can be applied to obtain sediment concentration, (Gippel 1995), in which case these two variables are related linearly. On the contrary, Cohen *et al*. (2005) indicated that is rarely the case in seasonal arid streams. Most relationships of turbidity-concentration mentioned in the introduction deal with concentrations of an mg/l or p.p.m (Lane and Sheridan 2002, Pfannkuche and Schmidt 2003, Zabaleta *et al*. 2007, Estrany *et al*. 2009, Kändler *et al*. 2009). Turbidity is employed as a surrogate for SSC, and as a regulatory tool for showing land-use disturbance and environmental protection. Turbidity and suspended material have a linear relation, however, turbidity can indicate non-linear responses to Particulate

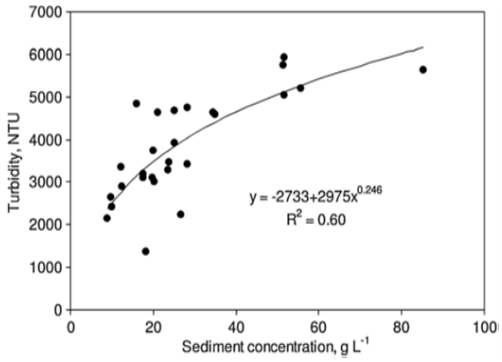

Fig. 2 Relationships between sediment concentration SSC and turbidity, NTU

Organic Matter (POM), concomitant with variations in Particle Size Distribution (PSD) (Bright *et al*. 2020).

2. Sediment-discharge formulas

Turbidity can be utilized to obtain sediment concentration since the researchers could not determine a set of sediment concentration measurements (C) that demonstrated the main source of sediment-discharge formulas. Some previous studies have pointed to the relationship between sediment concentration (mg/litre) and turbidity (NTU). However, this study will concentrate only on three equations.

2.1 Linear relationship (Gippel 1995)

There are several methods for investigation of linear relationship in engineering as experimental data can be expensive and time-consuming tests. In recent years, various techniques have been used for this purpose, such as artificial neural networks. Extreme learning machine, neural network, genetic programming and other functional networks are applied to predict and validate the experimental data. Moreover, finite element method is one of the reliable ways, which is utilized by researchers for response prediction (Arabnejad Khanouki *et al*. 2011, Daie *et al*. 2011, Sinaei *et al*. 2012, Mansouri *et al*. 2016, Sari *et al*. 2018, Shariati *et al*. 2019b, c, 2020e, Xu *et al*. 2019). Gippel (1995) studied the impact of particle size on Specific Turbidity (ST). It was reported that variation of particle size could change the turbidity by a factor of 4 for the same SSC. In addition, Gippel (1995) showed that for a turbid-meter which was calibrated to provide a linear response to a forming standard, the turbidity of a mix, which has a fixed grain size composition, will change linearly based on the following term

$$T = aKC_S + b \rightarrow 1 \quad (1)$$

where T, K and C_s show turbidity, specific turbidity and suspended solids concentration, respectively. Also, a = constant, which is a function of dissolved organic colour for NTU $a \leq 1$ and b = constant and is a function of organic colour, for NTU $b = 0$.

2.2 Nonlinear relationship (Lewis 1996)

Lewis (1996) develops the experimental relationship between turbidity as nephelometric turbid-meters (NTU) and Sediment Concentration (SC). The study was included (i) the linearity of the relationship when the grain size is constant and the greater ST corresponding the finer particles. A relatively small effect of larger sand-size particles on turbidity was seen, (ii) when particle size changes as a function of concentration, a nonlinear form of the turbidity response is obtained as follows

$$T = a.\, C_s^{c} + b \rightarrow 2 \quad (2)$$

where (a, b) are characteristic coefficients. When as a function of SSC, particle size increases, $c < 1$ and shows reducing ST, when particle size decreases as a function of concentration, $c > 1$.

2.3 Measurable relations (Polyakov et al. 2013)

A non-linear relationship between turbidity and total sediment concentration for all samples was obtained by Polyakov *et al*. (2013)

$$NTU = 2975 \times TC^{0.246} - 733 \rightarrow 3 \quad (3)$$

where NTU and TC are nephelometric turbidity units and Total concentration of sediment (in mg/l), respectively. This sort of non-linear relation between turbidly and concentration has been attributed to changes in sediment properties channel by sediment deposits. Furthermore, as shown in Fig. 2, a good relationship was seen from the turbidity measurements with total sediment concentration (R^2 = 0.60). Moreover, the relationship between sediment discharge and concentration (Q_S, C_S) commonly plotted as a function of water discharge (Q_w) on log-log paper, is named SRC. There are two types, which are commonly used in relationships. First, concentration (C_S) versus discharge (Q_w), and second, sediment load (Q_S) versus discharge (Q_w). Since SY is a product of both concentration and discharge, in the later curve, the discharge term reveals on both axis and makes an apparent fit, which is better than the original dataset. Field data plots indicate virtually immediate concentration-discharge data pairs. However, rating curves may also be plotted indicating average sediment concentration (C) or sediment load (Q_S) as a function of water discharge (Q_{water}) averaged over daily, monthly or other periods.

Additionally, in some streams, a single log-log relationship can characterize the concentration against the curve of discharge rating. In addition, a better relationship can be achieved by forming multiple curves to various model components of the total load, when there is a poor relationship between concentration and discharge. For example, separate curves may be provided for the coarse and fine size classes, for rising and falling stages, for summer and winter conditions, or for different discharge ranges. An inherent problem in the Rating Curve (RC) method is the high degree of scattering, which may be decreased but not eliminated.

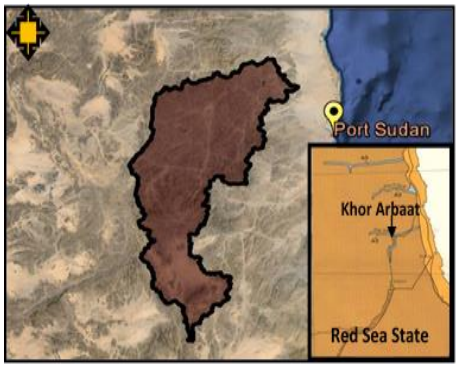

Fig. 3 Location map of study area

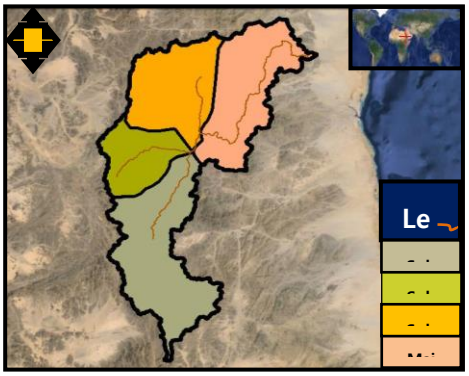

Fig. 4 Khor Arbaat streams and sub basins of drainage area

As a function of discharge, concentration does not necessarily increase. A high degree of scatter happens when processes control sediment delivery to the stream in the watershed that does not have a good correlation with the stream discharge. A good curve fit does not indicate a precise representation of the hydrologic process unless the entire range of discharges is covered by the data. The data includes both rising and falling stages of hydrographs from storms during all seasons, unusual hydrologic conditions do not bias the data, and the given data includes points at high discharge for more than a single event.

3. Materials and methods

3.1 Description of study area

The area of study is placed in the Red Sea state, in northeastern Sudan, about 50 km north of Port Sudan town, the state capital. Administratively, Arbaat is a part of the Red Sea locality, one of the six regions consisting of the Red Sea state. The area is the area catchment for Khor (small stream) Arbaat, after which it is named. The Khor crosses the area in an east-west direction during its flow from the Red Sea hills, where it begins, to the Red Sea where it discharges. The study area comprises of Red Sea state, Port Sudan town and Khor Arbaat. The Red Sea area of Sudan is extended from the Egyptian border in the north at latitude 22° 30" N to the Eritrean border in the south at 18° 00" N and from longitude 35° 00" E to the Red Sea coast

Table 1 Drainage areas of Khor Arbaat sub watersheds

Sub-watershed	Drainage area (km^2)	Perimeter (km)	Stream (km)	%
Main stream basin	1227	170	89.7	28
Sub-basin 1	1530	215	52.1	35
Sub-basin 2	600	101	36	14
Sub-basin 3	1030	150	25.4	23
Total	4387	506	203.2	100

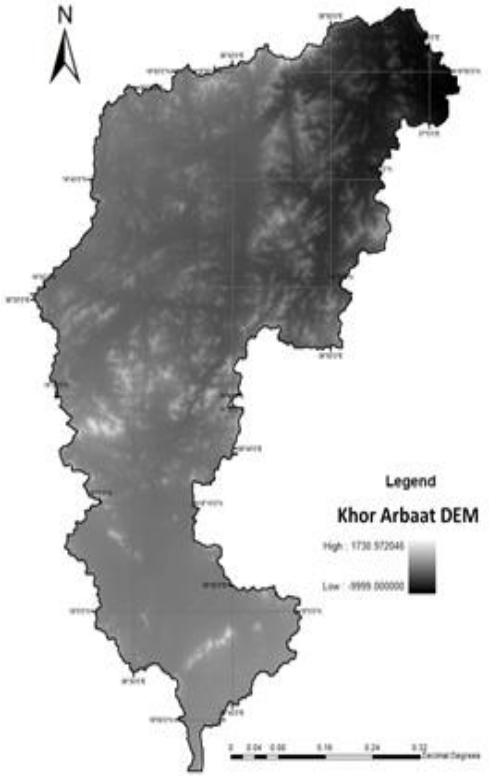

Fig. 5 Topographic map Khor of Arbaat watershed by Digital Elevation Model (DEM)

at 37° 15" E. The study area is located the central Red Sea state area around Port Sudan town, bounded by lat. 19° 55" N to 18° 45" N and long 36° 26" E to 37° 15" E. The location map is shown in Fig. 3. Khor Arbaat is known as the largest source of water near Port Sudan, which is located in the central Red Sea state (Fig. 3). The distance of this Khor to the city is about 50 km, and the Wadi has a length of 160 km including Wadi Odrus with the steep slope of 6-10 m per one kilometer. Khor Arbaat is the main source of water supply for Port Sudan city, which is the capital of the Red Sea state, and second city in Sudan after Khartoum. Khor Arbaat takes high flood in summer and winter seasons, but these quantities of water are useless. The large change in the average annual rainfall (ranging between 86 mm) has been seen for the area around Khor and the meteorological reports have measured at 6 mm for Red Sea area. At Port Sudan, the maximum annual rainfall (for about 50 years) is about 277 mm. Thus, the daily flow rates for the same

Table 2 Khor Arbaat catchment area maximum rainfall during 1944-2000

Max daily rainfall (mm)							
Port Sudan		Sinkat		Arbaat		Suakin	
Date	Rainfall	Date	Rainfall	Date	Rainfall	Date	Rainfall
30-11-1949	104	31-7-1944	82	10/11/1946	53	27/11/1947	84
20-12-1950	106	8-8-1952	101	21/12/1982	81	29/10/1958	50
6-11-1951	74	12-8-1953	71	-	-	24/12/1958	50
21-11-1957	111	24-10-1959	61	-	-	30/11/1961	85
30-11-1961	56	12-9-1959	61	-	-	29/11/1962	95
9-11-1962	51	17-8-1962	51	-	-	8/1/1963	90
20-11-1975	60	16-8-1967	51	-	-	27/11/1965	95
20-12-1978	56	-	-	-	-	30/10/1966	98
16-10-1979	58	-	-	-	-	20/11/1968	84
17-4-1993	138	-	-	-	-	28/10/1972	99
27-10-1997	163	-	-	-	-	-	-

Table 3 Maximum daily rainfall corresponding return period (*T*)

Return period (*T*, years)	Maximum rainfall (mm)			
	Port Sudan	Arbaat	Suakin	Sinkat
10	81.3	38.8	86.3	62.1
20	99.8	48.4	103.2	74.5
50	123.7	60.6	125.11	90.7
80	135.4	66.8	136.3	98.9
100	141.6	69.8	141.5	102.8
Gumbel's value distribution	Average = 38.4 mm S.D = 32.9 mm N = 57	Average = 16.9 mm S.D = 16.7 mm N = 32	Average = 46.9 mm S.D = 30.1 mm N = 29	Average = 33.1 mm S.D = 22.2 mm N = 32

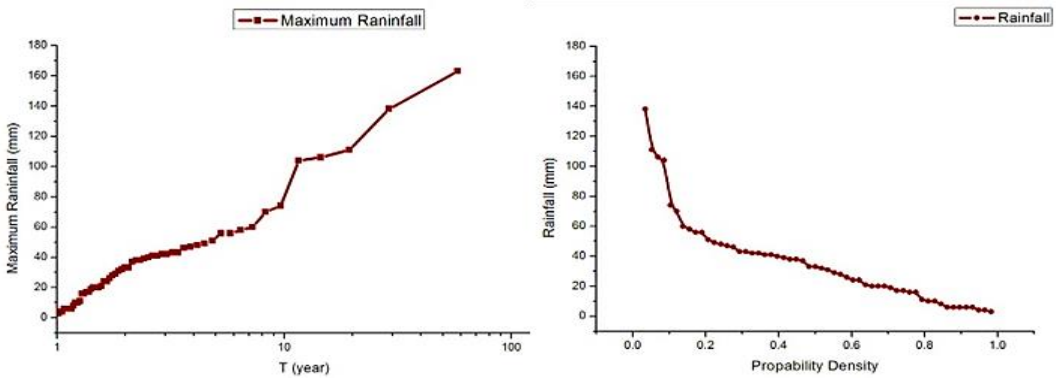

Fig. 6 Gumbel distribution for maximum daily rainfall data (PMP, T, P)

report has reached 1229 m^3/sec. About 4387 km^2 Catchments Area (CA) is drained by Khor Arbaat through the upper gate into the alluvial basin of lower gate, and these areas divide into four sub-basins. The CA of the Khor is by far the largest in this region. The CA of Khor Arbaat can be regarded very close to the shore area of Port Sudan.

The water supplies from Khor Arbaat are wells, baseflow and reservoirs. There are three dams: Fourth reservoirs, Sea Port Corporation Dam and Upper gate dam generally suffer siltation and their capacities storage decrease due to floodwater. Several studies have been considered in order to provide a sustainable water supply for the city by developing Khor Arbaat water resources through construction dams. Because of the siltation from the untreated Saraf and reservoirs water, capacities of storage reservoirs are losing. Siltation also leads to increasing the turbidity of water extracted from theses reservoirs and creates a favorable environment for

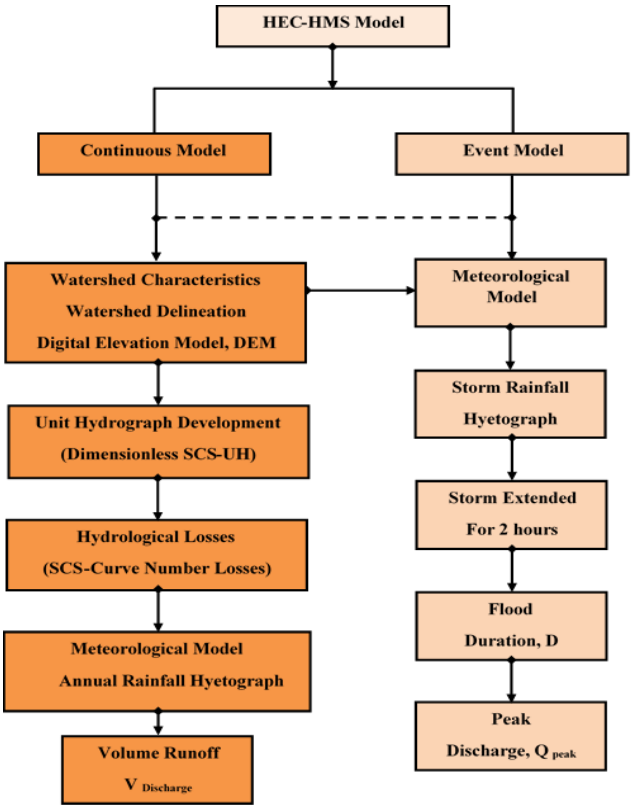

Fig. 7 HEC-HMS 3.5 Model Flowchart

anaerobic bacteria and other biomass to grow (Consult 2002). The watershed contains four major catchments see Fig. 4. Topographic relief changes significantly through the watershed. It descends gently from an elevation of 1730 to 10 m in the west eastwards to sea level in the vicinity borders of the Red sea. Fig. 5 depicts the topographic map (DEM) of Khor Arbaat Watershed.

3.2 Data collection and analysis

3.2.1 Rainfall data analysis

(i) Maximum rainfall events: In general, studying the extreme hydrological events required choosing the largest or smallest events. However, for rainfall-runoff hydrological modelling and sediment transport prediction, the researcher is more interested with the largest extreme events that have a large probability of creating maximum runoff. The Rainfall-runoff analysis using HEC-HMS model indicated that the surface-runoff in the Arbaat watershed occurs when rainfall exceeds 35 mm in one day or 50 mm in two consecutive days. Table 2 below shows the maximum daily rainfall for Port Sudan, Arbaat Suakin and Sinkat stations. Moreover, the maximum daily rainfall events were analyzed using frequency analysis. The main purpose of the frequency analysis of hydrological data is to relate the magnitude of extreme values to their frequency of occurrence through the use of probability distribution.

(ii) Depth-duration-frequency-intensity of Arbaat rainfall: In several hydraulic structures, such as those related to floods, the possibility of a particular, severe rainfall of specific duration will be significant. In general,

Table 4 Description of data entry for HEC-HMS 3.5

	Data entry for HEC-HMS 3.5	Description
1	Arbaat watershed characteristics	Fig. 8 shows the Khor Arbaat watershed delineation
2	Rainfall input data	113.9 mm in average values of stations and 141.6 as the maximum value
3	Hydrologic losses	Soil group A CN for arid and semi-arid conditions, soil group A and poor ground cover S = 5.87 in = 29.8 mm main-catchment
4	Time of concentration Tc and lag time T_{lag}	Fig. 9 shows the time of concentration, TC using GIS with an incremental time of 60 min (TC maximum = 6346.68 min)
5	Evaporation and transpiration losses	The evaporation and transpiration losses are not estimated in the event HEC-HMS model.

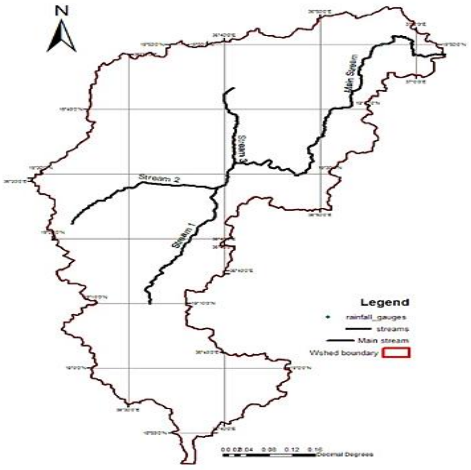

Fig. 8 Khor Arbaat watershed delineation

the rainfall duration can be categorized as (i) short duration, which is lasting from 1 minute to 1 hour, (ii) intermediate duration, from 1 to 24 hours, and (iii) long duration which is more than 24 hours. In arid and semi-arid zones like Arbaat area, which generally have short-duration rainfall, a maximum duration of 2 hours is suggested. The Depth-Duration-Frequency (DDF) relationships have a considerable effect on this investigation for estimation of the peak discharge (Q_{peak}) with HEC-HMS. Unfortunately, in the study area, the data for 24-hour of rainfall are available. Hence, a study of sediment prediction is constrained to either consider a uniform precipitation distribution over the total storm duration, which results in the underestimation of peak discharges or assuming the rainfall depth record for each storm by duration 120 minute (2 hours). For consistency, the Gumbel distribution was used for all frequency analysis in this study.

(iii) Gumbel's distribution: Gumbel distribution is one of the most widely used probability distribution functions

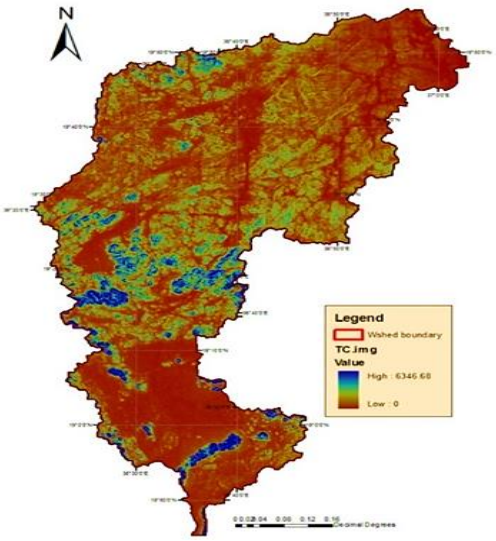

Fig. 9 Time of concentration using GIS

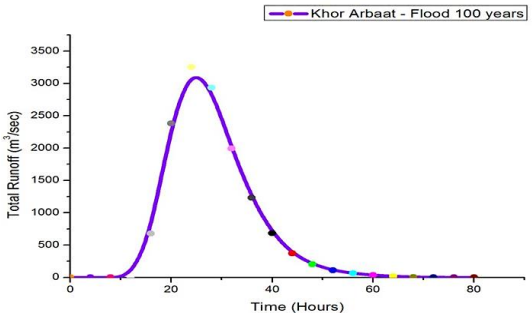

Fig. 10 Khor Arbaat flood using HEC-HMS run-simulation

for extreme values in hydrologic and meteorologic studies for prediction of maximum rainfall, flood peak (Soliman 2010). The calculation of maximum rainfall is essential for the computing Suspended Sediment Discharge (SSD) and then sediment bed load. For this purpose, the Gumbel method has been used for this research work. The daily maximum rainfall events for study area shown in Table 3, was found to be the suitable probability distribution for extreme value type 1. The relation between the annual maximum rainfall, X_T, and the corresponding return period T, for Arbaat watershed area, is given by Gumbel equation as PMP

$$X_T = 38.4 + 32.9\left(-ln\left(Ln\frac{T}{T-1}\right)\right) \rightarrow 5 \qquad (4)$$

The return period (T) of a design rainfall storm should be based on economic efficiency (ASCE 1992). However, in practice, the return period (T) is usually selected based on the level of hydraulic structures. It was found that the return period of 100 years from Table 3 provided rainfall value of 141.6 millimetres, which is almost the same as the PMP; as a result, 141.6 mm will be the value taken for HEC-HMS model.

(iv) Application of Gumbel distribution and Weibull formula: The Weibull formula, as shown in Eq. (5), was used for frequency analysis of rainfall where the probability of occurrence of an event whose magnitude is equal to or in excess of a specified magnitude X is denoted by P, as follow

$$P = \frac{m}{N+1}, \qquad T = \frac{N+1}{m} \qquad (5)$$

where P is the probability rainfall equaled or exceeded, T is the Return period (recurrence interval is given as: $T = 1/P$, m is the order number (m = 1, 2, 3, 4,..., N), in the last event $m = N$ = number of years on record, and N is the sample size (number of records).

The Gumbel's distribution formula given in Eq. (6) was also used to estimate the rainfall magnitude corresponding to a given return period based on a maximum daily rainfall (annual series)

$$X_T = \bar{x} + K_T\sigma_p \qquad (6)$$

where $\bar{x}$ is the mean value of the maximum rainfall data, σ_p is the standard deviation of the maximum rainfall data, and K_T is the frequency factor is expressed as type 1 distribution and can be calculated by the following Eq. (7).

$$K_T = -\frac{\sqrt{6}}{\pi}\left(0.5772 + ln\left(Ln\frac{T}{T-1}\right)\right) \qquad (7)$$

Gumbel extreme value frequency factors: K_{10} = 1.3, K_{20} = 1.9, K_{50} = 2.6, K_{80} = 2.96, K_{100} = 3.1.

The estimated return periods for maximum daily rainfall events of over 123.7 mm and 141.5 mm exceed 50 and 100 years, respectively. Besides, the maximum rainfall depth of p^2_{100} = 141.6 mm/day was found from the curves given in Fig. 6.

3.2.2 Rainfall-runoff models

In this study, HEC-HMS was used to predict runoff volume and peak discharge at Arbaat watershed. HEC-HMS is a computer program that includes a variety of models which are used to simulate the rainfall-runoff process. The HEC-HMS 3.5 model was developed for Khor Arbaat watershed to predict the flood peak (Q_{peak}). Fig. 7 presents the approach that is adopted to construct the HEC-HMS 3.5 model.

3.2.3 Data entry for HEC-HMS 3.5

Due to the lack of detailed values for maximum flow (Q_{peak}) and flood duration of Khor Arbaat as hydrology database, it is often necessary recourse to models by which the maximum volume discharge of the study area can be predicted based on its watershed characteristics and the maximum expected depth of rainfall as return period 100 years. Therefore, based on the data given in Table 4 and Figs. 8 and 9, HEC-HMS 3.5 was used for further analysis.

3.2.4 Output data from HEC-HMS 3.5

The simulation was applied in order to predict the total peak discharge generated from the maximum rainfall event. The results from applying the HEC-HMS 3.5 for the different input data are presented in Fig. 10 and Table 5. Based on the obtained results from HEC HMS Model simulating and analyzing of the flood for Khor Arbaat area,

Table 5 Flow discharge (m^3/sec) developed by HEC-HMS (output data)

No.	Time in hours	Runoff (m^3/s)
1	0	0
2	4	0
3	8	0
4	12	9.2
5	16	678.3
6	20	2379.8
7	24	3263.7
8	28	2934.3
9	32	1993.5
10	36	1229.7
11	40	684.4
12	44	372.9
13	48	205.4
14	52	112.6
15	56	62.3
16	60	35.2
17	64	16.6
18	68	5.3
19	72	1.6
20	76	0.2
21	80	0

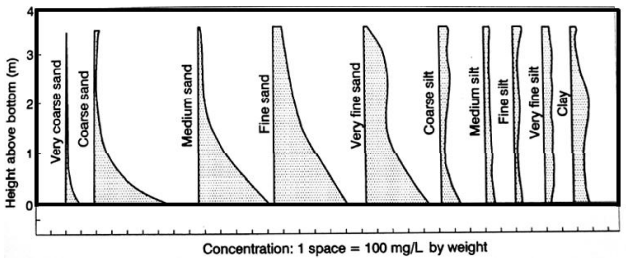

Fig. 11 Vertical variations in sediment concentration as a function of grain size

the peak discharge of 3263.7 m^3/sec, runoff volume of 201.058 × 10^3 m^3, and the duration of flood storm of 80 hours were noted.

4. Sediment data analysis

The available information for Wadi Arbaat region on sediment was limited. The sediment data collection and analysis are essential for the optimal control of the sediment transport on Wadi Arbaat sediment, as well as for the protection of the dams on the upper gate area. Therefore, the analyses include the sizes of sediment bed materials, the distribution of sediment bed materials through the area of sampling, and the pattern of deposition are presented and shown in this part.

Table 6 Maximum result of turbidity in water quality lab NTU

Turbidity (NTU)	Suspended solids mg/l	Permissible in drinking water and remarks
1535	560	Under 5 NTU high due to flood, Nil

4.1 Sediment monitoring station

There are no sediment monitoring stations installed along Khor Arbaat for measuring the sediment concentration entering the dams' reservoirs. Due to this reason, no data was available from Khor Arbaat related to SSC. Therefore, the turbidity NTU samples have great significance in this study.

4.2 Estimating suspended sediment concentration using turbidity data

Due to the lack of sediment concentration measurements (SSC) data in Khor Arbaat during the flood period, there are no historical records for suspended sediment. Turbidity is considerably affected by the transported sediment properties, such as size, shape and mineral composition. With frequent calibration, the relation of turbidity NTU to SSC could be used to estimate SLs more efficiently in this research. The details of turbidity-concentration relationships are mentioned in the literature and pointed out some conditions for the use of these equations.

Turbidity (NTU, FTU) may not be appropriate for representing total sediment loads in arid watersheds or seasonal streams such as Arbaat. However, if fine sediment is the primary interest, then the turbidity approach can be a practicable alternative. It also can be employed to fill the gaps in the data received by direct suspended sediment sampling. In the absence of any suspended sediment data, the estimation and prediction procedure of sediment concentration SSC reveal that examining the relationship between SSC and turbidity NTU values might be one efficient method for computing SSL in Arbaat watershed if the suspend sediment generally as fines materials (silt, clay), consequently, particles size less than (< 0.360 mm). Also, sediment particles along a vertical axis within the water column are almost uniform distribution.

Overall, these conditions are essential for turbidity sampling; when particle size decreases produce a relatively good result on turbidity as a function of concentration. In contrast, the larger sand-size particles create a relatively small result on turbidity as a function of concentration. According to Dendy *et al*. (1979), as shown in Fig. 11, the change in particle size, sediment concentration and velocity as a function of depth, indicating that the sediment concentration profile alters as a function of grain size, with large-diameter particles being concentrated closer to the bottom of the vertical profile.

Table 7 Sediment concentrations derived with turbidity values

Method	T (NTU)	Empirical equation	Coefficients	SSC (mg/l)
Gippel (1995)	1535	$T = a.K.C_s + b$	$a = 1$, $b = 0$, $k = 2.65$	579
Lewis (1996)	1535	$T = a.C_s^C + b$	$a = 1$, $b = 0$ $c = 1.2$	541
Polyakov *et al*. (2013)	1535	$T = 2975 \times TC^{0.246} - 733$	$a = 2975$, $b = -733$, $c = 0.246$	0.33
River Nile, (1999)	1535	$SSC = 4549.7 \times T - 125.56$ $R = 0.9441$	$a = 4549.7$, $b = -125$, $c = 1$	6983663.94

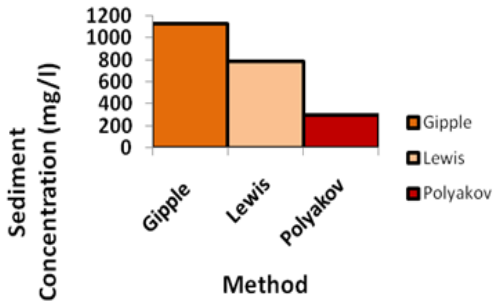

Fig. 12 Predicted sediment concentrations values of three methods

4.3 Maximum turbidity results and water quality analysis

Turbidity in water quality has been extensively utilized to identify the occurrence of pollutants in Khor Arbaat surface water. Surface water samples collected, showed the maximum value of turbidity of 1535 NTU at the area lying at about 3.5 km upstream from the upper-gate. These samples mixed with Saraf water. This indicates that the values of turbidity may be higher values than as shown in the below table. The values of turbidity recognized in this research (up to 1535 NTU) extend beyond the range where the light scattering technique is commonly used. Table 6 illustrates the maximum turbidity values used in this study for obtained sediment concentration.

4.4 Sediment concentration prediction in Arbaat

The SSC is considered as the ratio between the weights of the filtered matter of sediment with regard to the total sample weight. The SSCs are employed to estimate the sediment load. Using data collected from 1990 to June 2015 at the upper gate along Khor feeding the basin of Dam 1, the relationship between the concentrations of suspended sediment SSC and turbidity NTU was calibrated. Sediment concentration was determined by using linear relationship by Gippel (1995), experimental relationship by Lewis (1996), measurable relations by Polyakov *et al*. (2013) and NTU and SSC relationship in river Nile by Ministry of Irrigation (1999).

Table 8 Values of k for Q_s, Q_{flow} and C in units indicated

Q_s	Q_{flow}	C	k
English tons/day	ft^3/sec	mg/l	0.0027
metric tons/day	ft^3/sec	mg/l	0.0024
metric tons/day	m^3/sec	mg/l	0.0864
1 English ton = 2000 lb		1 metric ton = 1000 kg = 9810 N	

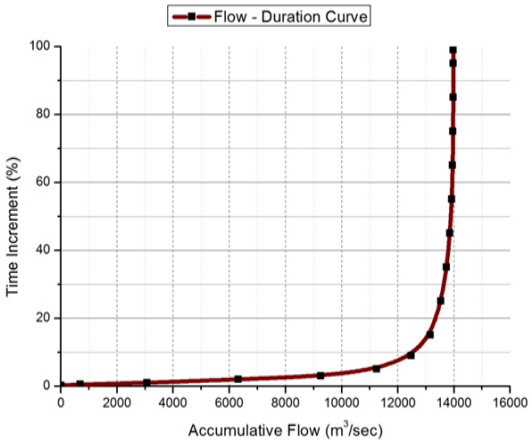

Fig. 13 Khor Arbaat flow-duration curve

The obtained results are given in Table 7 and Fig. 12 indicates that the linear regression equations of sediment concentration and turbidity provided a maximum result, with SSC = 1130 mg/l and the nonlinear minimum value SSC = 790 mg/l for three maximum turbidity data collected in Arbaat.

5. Suspended load discharge (Q_s)

In order to estimate the SSL, the information of concentration SSC and discharge in continuous form should be available. The daily SL is obtained as a product of the mean daily Suspended Matter Concentration (SMC) and daily average of discharge. While the daily discharge can be determined very merely, the daily concentration of the suspended solid is estimated more complicated, since the discontinuous sampling results in data gaps in the concentration hydrograph curve. Since the specimens are not taken continuously, larger flood events can be missed, which results in significant uncertainties by the estimation of the SSL. In order to better describe the discontinuous concentration measurements, the combination of these discontinuous concentration monitoring with the continuous turbidity measurements by the nephelometric device is done.

5.1 Sediment-discharge formulas

The beginning of the first attempts to develop a sediment discharge formula in rivers is back to Du Boys, in1879. During the twentieth century, a great many sediment- discharge formulas were proposed; several of

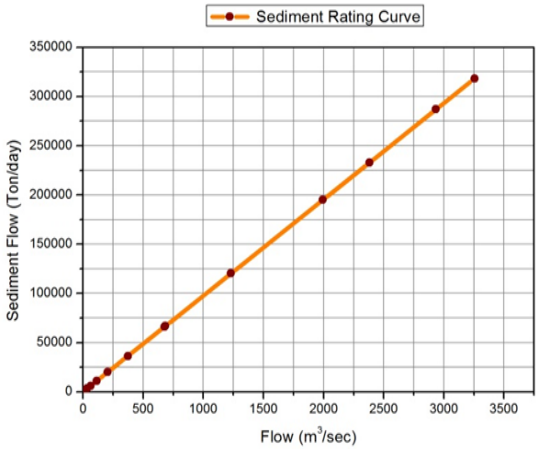

Fig. 14 Khor Arbaat sediment-rating curve

those have been extensively used. The famous hydraulic engineers, whose names are, associated with sediment-discharge formulas, 1) Einstein Hans Albert, 2) Meyer-Peter and Muller, 3) Bagnold, 4) England and Hansen (Marcelo H. Garcia, 2006). This study is not the place to describe the various widely used suspended sediment-discharge formulas. Therefore, this research will concentrate only on the formula below, which is converts from concentration to sediment discharge

$$Q_s = f(Q_{flow}) \rightarrow Q_s = \text{K.C.}Q_{flow} \quad (8)$$

where Q_S is the sediment discharge (suspended sediment transport) (tons/day); K = 0.0027, when other variables are expressed in designated unit; C is the concentration (mg/l); Q is the water discharge (m^3/s).

5.2 Data required for determining suspended-sediment

In general, the most important data collected to determine the SSD of a watercourse are as follow:

(i) Water discharge (Q_{flow}): It is the immediate water discharge in (m^3/sec). This quantity is either measured with a current meter or obtained from a stage-discharge curve for the gauging station. Due to no data of flows obtained from Khor Arbaat, all discharges were predicted from Rainfall-runoff model called HEC-HMS 3.5 model as maximum monthly flow.

(ii) Sediment concentration data (C): Sediment concentration is the weight of dry sediment in a water-sediment mixture per volume of the mixture and is represented in milligrams/litre (mg/l) or parts of sediment per million parts of water (p.p.m). By analysing the water samples, concentration is measured. To estimate SSC in Khor Arbaat, turbidity values obtained in 2005 are used. For low sediment concentrations (< 15,000 p.p.m), the concentration in mg/l is the same as that in p.p.m. For concentrations greater than 15,000 p.p.m, the conversion factors in Annex C.3 is used. The conversion factors can be applied to turn p.p.m into mg/l.

(iii) Sediment discharge (Q_s): Sediment discharge also called the Sediment transport rate; sediment discharge is the quantity of sediment per unit of time passing a cross-section it is represented as tons/day. Besides, the sediment discharge (Q_s) is expressed in terms of weight or terms of volume rather than in terms of mass.

(iv) Conversion factor (K): The conversion factor is indicated by K, which is appropriate to the units utilized for Q_{flow}, C and Q_s. The different values of K are given in Table 8.

This study used all the dimensions of the above data required as follow, Q_{flow} in m^3/sec, Q_s in metric ton/day, C in mg/l; therefore, the conversion factor value K was taken equal to 0.0864.

$$Q_s = 0.0864.\text{C}.Q_{flow} \quad (9)$$

5.3 Methods for estimating suspended-sediment discharge

From the above formula, when the values of water discharge (Q_{flow}) and suspended -sediment concentration C are known, two techniques are available for the estimation of SSD in this research as follow.

5.3.1 The concentration graph - hydrograph method

It is the most precise approach to compute SSL, although it is also complicated and needs the most complete and detailed discharge (Q_{flow}) and sediment data (sediment sampling). It is particularly suitable for estimating the sediment discharge (Q_s) throughout storm where there has been thorough sampling over the entire hydrograph. This method is tough or impossible to apply in this research because the SSCs data on the Khor Arbaat are insufficient.

5.3.2 Duration curve and sediment rating curve method

This is a suitable approach to estimate the sediment discharge on a stream. It is especially appropriate in the case, where we have only predicted peak discharge and turbidly sediment data, that is to say, where a discontinuous sampling is available. This method could be applied to calculate suspended-sediment or bed load discharges. The calculations of this method are best done using a table and excel-sheet OrignPro8. Moreover, the procedure description explains the approach adopted in the estimation of the annual SSD (ton/year) carried by the Khor were in few steps. First, construct the Flow-Duration Curve (FDC) for the stream, as shown in Fig. 13. In this case, study, which is the cumulative distribution curve of Khor Arbaat passing the dam. The researcher used a program of HEC-HMS for predicting the peak of daily discharge (Q_{water}). Second, plot the sediment rating- curve for upper gate site, as illustrated in Fig. 14, which relates sediment concentration SSC to Khor Arbaat discharge (Q_{water}) passing upper gate area. Fit the data with a straight line or a smooth curve, whichever appears more appropriate by using OriginPro8. The turbidity data as nephelometers were reading Arbaat water quality analysis used to determine sediment concentration for flood season.

In this study, to evaluate the SSD for Khor Arbaat, six different parameters have been assessed and named as Ray 1 to Ray 6. Ray 1, which divides the FDC into equally

Table 9 Suspended-sediment discharge for Khor Arbaat

Ray 1		Ray 2	Ray 3	Ray 4	Ray 5	Ray 6
% Time increment		Time in increment	Average of time increment	Daily flow (Q_{flow})	D.S.F (Q_s)	S.S.D for time increment
	%	Δ %	%	m^3/sec	Ton/day	Ton
1	0.02	0.02	0.01	9.2	460.24	0.37
2	0.1	0.08	0.06	678.3	33932.4	33.93
3	0.2	0.10	0.15	2379.8	119051	357.2
4	0.5	0.30	0.40	3255.6	162863.3	814.32
5	1.0	0. 5	0.75	2934.3	146790.1	1467.90
6	2.0	1.0	1.5	1993.5	99726.03	997.3
7	3.0	1.0	2.5	1229.7	61516.5	1230.33
8	5.0	2.0	4.0	684.4	34237.5	1369.50
9	9.0	4.0	7.0	372.9	18654.5	1119.3
10	15.0	6.0	12.0	205.4	10275.3	1027.53
11	25.0	10.0	20.0	112.6	5632.9	563.3
12	35.0	10.0	30.0	62.3	3116.6	311.7
13	45.0	10.0	40.0	35.2	1760.9	176.1
14	55.0	10.0	50.0	16.6	830.4	83.04
15	65.0	10.0	60.0	5.3	265.14	26.5
16	75.0	10.0	70.0	1.6	80.04	8.00
17	85.0	10.0	80.0	0.2	10.01	1.00
18	95.0	10.0	90.0	-	-	-
19	99.0	4.0	97.5	-	-	-
20	99.8	0.8	99.4	-	-	-
	Total	99.8	-	-	-	9587.12

• Average daily suspended sediment load: 9587.12 tons/day
• Total annual suspended sediment load: 9587.12 × 60 day/year = 575227.2 ton/year, 977886.24 m^3/year
• 980000 m^3/year (according to the decreasing of storage of U/S UG Dam 1)

Table 10 Khor Arbaat total annual suspended sediment load (ton)

Method	Concentration (mg/l)	Average daily suspended sediment load	Annual suspended (ton)		
			60 day	90 day	120 day
Gippel (1995)	579	9587.12	57427.2	862840.8	1150454.4
Lewis (1995)	541	8957.95	537477	806215.5	1074954
Polyakov (2011)	0.33	5.5	330	491.77656	655.7

Table 11 Khor Arbaat bed materials samples analysis (classification and distribution)

Depth (m)	Description of sediment samples											
	1	2	3	4	5	6	7	8	9	10	11	12
0.0	Silty-clay	Gravelly sand	Sandy gravel	Fine sand	Sandy gravel	Sandy gravel	Fine sand	Gravelly sand	Sandy soil	Clay	Silt	Silty-clay

spaced sections of percentages. In this study, 20 sections-of-time intervals were selected as 1, 2, 3, 5, 9, 15, 25, 35, 45, 55, 65, 75, 85, 95, 99 and 99.8%, as given in Table 9. Therefore, from each equally spaced sections of percentages determine the duration of spaced section or increment (Δ % of the time), which called Ray 2. Ray 3 indicates the median time % of increment from Ray 2. The average discharge of water the Q_i corresponding to each median time (%) in Ray 3 was evaluated as Ray 4. Ray 5 indicates the D.S.F (Q_s), which found from the SRC, read the sediment concentration discharge Q_s, C_i corresponding to each average discharge of water Q_{flow} in ray 4. Finally, Ray6 specify the contribution of each time increment to the mean Daily Sediment Discharge (DSD) by multiplying each

Table 12 Khor Arbaat bed load estimation as three scenarios

Scenarios	SSC, mg/l	Stream bed material	The texture of suspended material	Bed load as suspended %	Total bed load (ton/year)
Scenario 1	1000-7500	Sand	20-50% Sand	10-35	57522.72-201329.52
Scenario 2	> 7500	Not Sand*	< 25%	5-15	28761.36-86284.08
Scenario 3	Any concentration	Clay and Silt	No Sand	< 2	< 115045.44

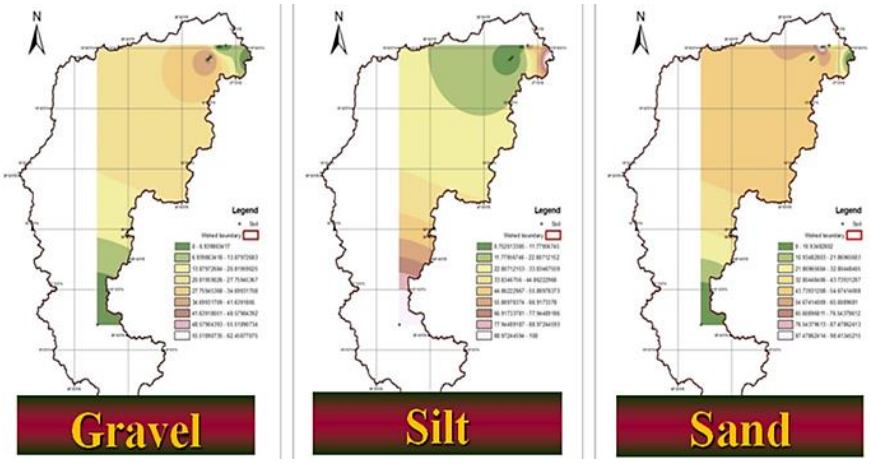

Fig. 15 Spatial distribution of Khor Arbaat bed materials (gravel, sand, silt)

Q_s in Ray 5 by the % time in the equivalent increment in column 2 and dividing by 100.

As the Ray 6 is summed, the abovementioned steps were repeated for each section to compute the average daily SSL (ton/day) in Khor Arbaat. This is the maximum DSD for the period demonstrated in the duration curve. Consequently, the average total SSL in Khor Arbaat in tons for the period of flood months were computed by multiplying the daily SSD by the total number of days in the period. Most rainfall and occasional intense storms occur in Arbaat watershed during June, July, August and September and may produce quite high rainfall. Winter rainfalls which happen due to costal rain also bring sediment but fewer amounts than those of the summer. Therefore, the numbers of days will be taken in this study for approximately 60 days. In addition, the total annual SSL (ton) for Khor Arbaat are given in Table 10.

6. Estimating the sediment bed load (Q_b)

In this study, the bed load (Q_b) was not measured due to the difficulty of obtaining accurate field sediment-bed transport data in Khor Arbaat. However, the researcher relies on analysis data. Then, Q_b can be determined as a fraction of the suspended sediment discharge Q_s. The researcher used Strand and Pemberton (1987) procedure outlined in the literature review for estimating bed load or bed-material load. This procedure is predicated on the presence of specific relations among hydraulic variables of (i) SSC mg/l, (ii) suspended material texture, distribution of fine materials (%), (iii) stream bed materials, particle size distribution curve (mm) and (iv) bed material load transport rate at steep slopes. Table 11 developed to estimate the sediment bedload Q_b, which resulted from applying the Strand and Pemberton empirical procedure to Khor Arbaat case study. Besides, Table 12 illustrates the three scenarios according to Fig. 15 and the data given in Table 11. Based on observation during site visits, sediment bed materials analysis, the spatial interpolation IDW tool in GIS for sand distribution in the bed of the Khor, and total sediment concentration SSC values derived by nephelometric turbidity, Scenario 1 can be adopted. Moreover, the other studies also observed in semi-arid with a steep bed. For example, in the study by Frey (2011), the bed load was found, varying from 5 to 25% of suspended sediment transport. The SL during a flash flood in the semi-arid zone represents 60% for a stream from total sediment load (40% as bed load). Besides, the ratio of suspended sediment (Q_s) and bed load (Q_b) discharges in sand-bed streams form semi-arid region varied from 4% to 12.72% and the greatest values were recorded in the period of most considerable flow rates during the rainy season. By taking the bed load (coarse grain) as 35% of the discharge of the suspended material then the total sediment load for an average year is 776556.72 ton/year.

7. Conclusions

In this study, the turbidity data NTU in water quality has been used to the prediction of SSC in the estimation of suspended SY transport of Wadi Arbaat in Eastern Sudan. As there were no sediment monitoring stations installed along the Khor Arbaat region for measuring the sediment concentration entering the dams' reservoirs; therefore, the

turbidity NTU samples were used in the current study. Therefore, the data of concentration SSC and discharge in continuous form should be accessible in order to estimate the SSL. The daily-SL is obtained as a product of the mean daily of the SMC and the daily average of discharge. Besides, obtained results demonstrate the estimation of sediment load inflow using empirical formulas and assumptions, which calculates the SL of sediment in Khor Arbaat using FDC-SAC method and the bed load using the Strand and Pemberton Procedure (25-40% as SL). Besides, the total sediment load is essential for the optimal control of the sediment transport on Khor Arbaat sediment, and also for the protection of the dams on the upper gate area. Moreover, the study reveals an effective application of the turbidity NTU samples to predict the total sediment load.

Acknowledgments

This work was supported by the Deanship of Scientific Research at Prince Sattam Bin Abdulaziz University under the research project No 2019/01/1087.

References

Afrazi, M., Mahmoud, Y., Alitalesh, M. and Fakhimi, A.A. (2018), "Numerical analysis of effective parameters in direct shear test by hybrid discrete - finite element method", *Modares Civ. Eng. J.*, **18**(3), 13-24.

Afrazi, M. and Rouhanifar, S. (2019), "Experimental study on mechanical behavior of sand-rubber mixtures", *Modares Civ. Eng. J*, **19**(4), 83-96.

Alabduljabbar, H., Haido, J.H., Alyousef, R., Yousif, S.T., McConnell, J., Wakil, K. and Jermsittiparsert, K. (2020), "Prediction of the flexural behavior of corroded concrete beams using combined method", *Structures*, **25**, 1000-1008. https://doi.org/10.1016/j.istruc.2020.03.057.

Alaskar, A., Wakil, K., Alyousef, R., Jermsittiparsert, K., Ho, L.S., Alabduljabbar, H., Alrshoudi, F. and Mohamed, A.M. (2020), "Computational analysis of three dimensional steel frame structures through different stiffening members", *Steel Compos. Struct.*, *Int. J.*, **35**(2), 187-197. http://doi.org/10.12989/scs.2020.35.2.187.

Alyousef, R., Alabduljabbar, H., Mohamed, A.M., Alaskar, A., Jermsittiparsert, K. and Ho, L.S. (2020), "A model to develop the porosity of concrete as important mechanical property", *Smart Struct. Syst.*, *Int. J.*, **26**(2), 147-156. https://doi.org/10.12989/sss.2020.26.2.147.

Arabnejad Khanouki, M.M., Ramli Sulong, N.H. and Shariati, M. (2010), "Investigation of seismic behaviour of composite structures with concrete filled square steel tubular (CFSST) column by push-over and time-history analyses", *Proceedings of the 4th International Conference on Steel and Composite Structures*, Seoul, Korea, December.

Arabnejad Khanouki, M.M., Ramli Sulong, N.H. and Shariati, M. (2011), "Behavior of through beam connections composed of CFSST Columns and steel beams by finite element studying", *Adv. Mater. Res.*, **168**, 2329-2333. http://dx.doi.org/10.4028/www.scientific.net/AMR.168-170.2329.

Armaghani, D.J., Mirzaei, F., Shariati, M., Trung, N.T., Shariati, M. and Trnavac, D. (2020), "Hybrid ANN-based techniques in predicting cohesion of sandy-soil combined with fiber", *Geomech. Eng., Int. J.*, **20**(3), 191-205. https://doi.org/10.12989/gae.2020.20.3.191.

ASCE (1992), "Design and construction of urban stormwater management systems", ASCE and Water Environment Federation, USA.

Bright, C., Mager, S. and Horton, S. (2020), "Response of nephelometric turbidity to hydrodynamic particle size of fine suspended sediment", *Int. J. Sed. Res.*, **35**(5), 444-454. https://doi.org/10.1016/j.ijsrc.2020.03.006.

Cao, Y., Fan, Q., Azar, S.M., Alyousef, R., Yousif, S.T., Wakil, K., Jermsittiparsert, K., Ho, L.S., Alabduljabbar, H. and Alaskar, A. (2020a), "Computational parameter identification of strongest influence on the shear resistance of reinforced concrete beams by fiber reinforcement polymer", *Structures*, **27**, 118-127. https://doi.org/10.1016/j.istruc.2020.05.031.

Cao, Y., Wakil, K., Alyousef, R., Jermsittiparsert, K., Ho, L.S., Alabduljabbar, H., Alaskar, A., Alrshoudi, F. and Mohamed, A.M. (2020b), "Application of extreme learning machine in behavior of beam to column connections", *Structures*, **25**, 861-867. https://doi.org/10.1016/j.istruc.2020.03.058.

Cao, Y., Wakil, K., Alyousef, R., Yousif, S.T., Jermsittiparsert, K., Ho, L.S., Alabduljabbar, H., Alaskar, A., Alrshoudi, F. and Mohamed, A.M. (2020c), "Computational earthquake performance of plan-irregular shear wall structures subjected to different earthquake shock situations", *Earthq. Struct.*, *Int. J.*, **18**(5), 567-580. https://doi.org/10.12989/eas.2020.18.5.567.

Cohen, H. and Laronne, J.B. (2005), "High rates of sediment transport by flashfloods in the Southern Judean Desert, Israel", *Hydrol. Processes*, **19**(8), 1687-1702. https://doi.org/10.1002/hyp.5630.

Consult, S. (2002), "Ministry of housing and public utilities, Red Sea state water corporation, Khor Arbaat U/S upper gate dam, study and design final report", USA Ministry of Housing, USA.

Daie, M., Jalali, A., Suhatril, M., Shariati, M., Arabnejad Khanouki, M.M., Shariati, A. and Kazemi-Arbat, P. (2011), "A new finite element investigation on pre-bent steel strips as damper for vibration control", *Int. J. Phys. Sci.* **6**(36), 8044-8050. https://doi.org/10.5897/ijps11.1585.

Dendy, F., Alan, P., Piest, R., Brakensiek, D., Osborne, H. and Rawls, W. (1979), "Sedimentation: Field manual for research in agricultural hydrology", *USDA, Agr. Handbook*, **224**, 239-394.

Doğan, E., Yüksel, İ. and Kişi, Ö. (2007), "Estimation of total sediment load concentration obtained by experimental study using artificial neural networks", *Environ. Fluid Mech.*, **7**(4), 271-288. https://doi.org/10.1007/s10652-007-9025-8.

Duan, J.G. (2013), "A simple total sediment load formula", *Proceedings of the World Environmental and Water Resources Congress 2013: Showcasing the Future*, Ohio, USA, May. https://doi.org/10.1061/9780784412947.190.

Edwards, T.K., Glysson, G.D., Guy, H.P. and Norman, V.W. (1999), "Field methods for measurement of fluvial sediment", US Geological Survey Denver, Colorado, USA.

Estrany, J., Garcia, C. and Batalla, R.J. (2009), "Suspended sediment transport in a small Mediterranean agricultural catchment", *Earth Surf. Process. Landforms*, **34**(7), 929-940. https://doi.org/10.1002/esp.1777.

Fanaie, N., Aghajani, S. and Shamloo, S. (2012), "Theoretical assessment of wire rope bracing system with soft central cylinder", *Proceedings of the 15th World Conference on Earthquake Engineering*, Lisbon, Portugal, September.

Fanaie, N. and Dizaj, E.A. (2014), "Response modification factor of the frames braced with reduced yielding segment BRB", *Struct. Eng. Mech., Int. J.*, **50**(1), 1-17. https://doi.org/10.12989/sem.2014.50.1.001.

Fanaie, N., Esfahani, F.G. and Soroushnia, S. (2015a), "Analytical study of composite beams with different arrangements of channel shear connectors", *Steel Compos. Struct., Int. J.*, **19**(2), 485-501. https://doi.org/10.12989/scs.2015.19.2.485.

Fanaie, N. and Shamlou, S.O. (2015b), "Response modification factor of mixed structures", *Steel Compos. Struct., Int. J.*, **19**(6), 1449-1466. https://doi.org/10.12989/scs.2015.19.6.1449.

Fanaie, N., Aghajani, S. and Afsar Dizaj, E. (2016a), "Strengthening of moment-resisting frame using cable-cylinder bracing", *Adv. Struct. Eng.*, **19**(11), 1736-1754. https://doi.org/10.1177/1369433216649382.

Fanaie, N., Aghajani, S. and Dizaj, E.A. (2016b), "Theoretical assessment of the behavior of cable bracing system with central steel cylinder", *Adv. Struct. Eng.*, **19**(3), 463-472. https://doi.org/10.1177/1369433216630052.

Frey, P. (2014), "Particle velocity and concentration profiles in bedload experiments on a steep slope", *Earth Surf. Process. Landf.*, **39**(5), 646-655. https://doi.org/10.1002/esp.3517.

Gippel, C.J. (1995), "Potential of turbidity monitoring for measuring the transport of suspended solids in streams", *Hydrol. Process.*, **9**(1), 83-97. https://doi.org/10.1002/hyp.3360090108.

Haghnazar, H., Sangsefidi, Y., Mehraein, M. and Tavakol-Davani, H. (2020), "Evaluation of infilling and replenishment of river sand mining pits", *Environ. Earth Sci.*, **79**(14), 1-18. https://doi.org/10.1007/s12665-020-09106-z.

Jalali, A., Daie, M., Nazhadan, S.V.M., Kazemi-Arbat, P. and Shariati, M. (2012), "Seismic performance of structures with pre-bent strips as a damper", *Int. J. Phys. Sci.*, **7**(26), 4061-4072. https://doi.org/10.5897/IJPS11.1324.

Kändler, M. and Seidler, C. (2009), "Hydrochemical load in a small river following heavy rain events", *Folia Geograph.*, **40**, 27-32.

Katebi, J., Shoaei-parchin, M., Shariati, M., Trung, N.T. and Khorami, M. (2019), "Developed comparative analysis of metaheuristic optimization algorithms for optimal active control of structures", *Eng. Comput.*, **36**, 1539-1558. https://doi.org/10.1007/s00366-019-00780-7.

Khorami, M., Alvansazyazdi, M., Shariati, M., Zandi, Y., Jalali, A. and Tahir, M. (2017a), "Seismic performance evaluation of buckling restrained braced frames (BRBF) using incremental nonlinear dynamic analysis method (IDA)", *Earthq. Struct., Int. J.*, **13**(6), 531-538. http://dx.doi.org/10.12989/eas.2017.13.6.531.

Khorami, M., Khorami, M., Motahar, H., Alvansazyazdi, M., Shariati, M., Jalali, A. and Tahir, M.M. (2017b), "Evaluation of the seismic performance of special moment frames using incremental nonlinear dynamic analysis", *Struct. Eng. Mech.*, **63**(2), 259-268. https://doi.org/10.12989/sem.2017.63.2.259.

Lane, P.N.J. and Sheridan, G.J. (2002), "Impact of an unsealed forest road stream crossing: water quality and sediment sources", *Hydrol. Process.*, **16**(13), 2599-2612. https://doi.org/10.1002/hyp.1050.

Lewis, J. (1996), "Turbidity-controlled suspended sediment sampling for runoff-event load estimation", *Water Resour. Res.*, **32**(7), 2299-2310. https://doi.org/10.1029/96WR00991.

Liu, C., Wu, X., Wakil, K., Jermsittiparsert, K., Ho, L.S., Alabduljabbar, H., Alaskar, A., Alrshoudi, F., Alyousef, R. and Mohamed, A.M. (2020), "Computational estimation of the earthquake response for fibre reinforced concrete rectangular columns", *Steel Compos. Struct.*, **34**(5), 743-767. https://doi.org/10.12989/scs.2020.34.5.743.

Majedi, M., Afrazi, M. and Fakhimi, A. (2020a), "FEM-BPM simulation of SHPB testing for measurement of rock tensile strength", *Proceedings of the 54th US Rock Mechanics/ Geomechanics Symposium*, Colorado, USA, July.

Majedi, M.R., Afrazi, M. and Fakhimi, A. (2020b), "A micromechanical model for simulation of rock failure under high strain rate loading", *Int. J. Civ. Eng.*, **2020**, 1-15. https://doi.org/10.1007/s40999-020-00551-2.

Mansouri, I., Safa, M., Ibrahim, Z., Kisi, O., Tahir, M.M., Baharom, S.B. and Azimi, M. (2016), "Strength prediction of rotary brace damper using MLR and MARS", *Struct. Eng. Mech., Int. J.*, **60**(3), 471-488. https://doi.org/10.12989/sem.2016.60.3.471.

Mansouri, I., Shariati, M., Safa, M., Ibrahim, Z., Tahir, M. and Petković, D. (2019), "Analysis of influential factors for predicting the shear strength of a V-shaped angle shear connector in composite beams using an adaptive neuro-fuzzy technique", *J. Intell. Manuf.*, **30**(3), 1247-1257. https://doi.org/10.1007/s10845-017-1306-6.

McCully, P. (1996), *Silenced Rivers: The Ecology and Politics of Large Dams*, Zed Books, London, UK.

Milovancevic, M., Marinović, J.S., Nikolić, J., Kitić, A., Shariati, M., Trung, N.T., Wakil, K. and Khorami, M. (2019), "UML diagrams for dynamical monitoring of rail vehicles", *Physica A*, **531**, 121169. https://doi.org/10.1016/j.physa.2019.121169.

Moghaddam, H., Fanaie, N. and Hamzehloo, H. (2009), "Uniform hazard response spectra and ground motions for Tabriz", *J. Sci. Iran.*, **16**(3), 238-248.

Mohammadhassani, M., Nezamabadi-Pour, H., Suhatril, M. and Shariati, M. (2013), "Identification of a suitable ANN architecture in predicting strain in tie section of concrete deep beams", *Struct. Eng. Mech., Int. J.*, **46**(6), 853-868. https://doi.org/10.12989/sem.2013.46.6.853.

Mohammadhassani, M., Nezamabadi-Pour, H., Suhatril, M. and Shariati, M. (2014), "An evolutionary fuzzy modelling approach and comparison of different methods for shear strength prediction of high-strength concrete beams without stirrups", *Smart Struct. Syst., Int. J.*, **14**(5), 785-809. https://doi.org/10.12989/sss.2014.14.5.785.

Mohammadhassani, M., Saleh, A., Suhatril, M. and Safa, M. (2015), "Fuzzy modelling approach for shear strength prediction of RC deep beams", *Smart Struct. Syst., Int. J.*, **16**(3), 497-519. https://doi.org/10.12989/sss.2015.16.3.497.

Morris, G.L. and Fan, J. (1997), *Reservoir Sedimentation Handbook*, McGraw-Hill, New York, USA.

Morris, G.L. and Fan, J. (1998), *Reservoir Sedimentation Handbook: Design and Management of Dams, Reservoirs and Watersheds for Sustainable Use*, McGraw Hill Professional, New York, USA.

Okcu, D., Pektas, A.O. and Uyumaz, A. (2016), "Creating a non-linear total sediment load formula using polynomial best subset regression model", *J. Hydrol.*, **539**, 662-673. https://doi.org/10.1016/j.jhydrol.2016.04.069.

Pfannkuche, J. and Schmidt, A. (2003), "Determination of suspended particulate matter concentration from turbidity measurements: particle size effects and calibration procedures", *Hydrol. Process.*, **17**(10), 1951-1963. https://doi.org/10.1002/hyp.1220.

Polyakov, V., Nearing, M., Hawdon, A., Wilkinson, S. and Nichols, M. (2013), "Comparison of two stream gauging systems for measuring runoff and sediment yield for a semi-arid watershed", *Earth Surf. Process. Landf.*, **38**(4), 383-390.

Qi, C.C. (2020), "Big data management in the mining industry", *Int. J. Miner. Metall. Mater.*, **27**(2), 131-139. https://doi.org/10.1007/s12613-019-1937-z.

Rouhanifar, S., Afrazi, M., Fakhimi, A. and Yazdani, M. (2020), "Strength and deformation behaviour of sand-rubber mixture", *Int. J. Geotech. Eng.*, **2020**, 1-15. https://doi.org/10.1080/19386362.2020.1812193.

Sadeghipour Chahnasir, E., Zandi, Y., Shariati, M., Dehghani, E., Toghroli, A., Mohamed, E.T., Shariati, A., Safa, M., Wakil, K. and Khorami, M. (2018), "Application of support vector machine with firefly algorithm for investigation of the factors affecting the shear strength of angle shear connectors", *Smart Struct. Syst., Int. J.*, **22**(4), 413-424. http://dx.doi.org/10.12989/sss.2018.22.4.413.

Safa, M., Shariati, M., Ibrahim, Z., Toghroli, A., Baharom, S.B., Nor, N.M. and Petkovic, D. (2016), "Potential of adaptive neuro

fuzzy inference system for evaluating the factors affecting steel-concrete composite beam's shear strength", *Steel Compos. Struct.*, *Int. J.*, **21**(3), 679-688. https://doi.org/10.12989/scs.2016.21.3.679.

Safa, M., Maleka, A., Arjomand, M.A., Khorami, M. and Shariati, M. (2019), "Strain rate effects on soil-geosynthetic interaction in fine-grained soil", *Geomech. Eng.*, *Int. J.*, **19**(6), 533-542. https://doi.org/10.12989/gae.2019.19.6.533.

Safa, M., Sari, P.A., Shariati, M., Suhatril, M., Trung, N.T., Wakil, K. and Khorami, M. (2020), "Development of neuro-fuzzy and neuro-bee predictive models for prediction of the safety factor of eco-protection slopes", *Physica A*, **550**, 124046. https://doi.org/10.1016/j.physa.2019.124046.

Sari, P.A., Suhatril, M., Osman, N., Mu'azu, M., Dehghani, H., Sedghi, Y., Safa, M., Hasanipanah, M., Wakil, K. and Khorami, M. (2018), "An intelligent based-model role to simulate the factor of safe slope by support vector regression", *Eng. Comput.*, **2018**, 1-11. https://doi.org/10.1007/s00366-018-0677-4.

Sedghi, Y., Zandi, Y., Shariati, M., Ahmadi, E., Moghimi Azar, V., Toghroli, A., Safa, M., Tonnizam Mohamad, E., Khorami, M. and Wakil, K. (2018), "Application of ANFIS technique on performance of C and L shaped angle shear connectors", *Smart Struct. Syst.*, *Int. J.*, **22**(3), 335-340. https://doi.org/10.12989/sss.2018.22.3.335.

Shariati, M. (2020), "Evaluation of seismic performance factors for tension-only braced frames", *Steel Compos. Struct.*, *Int. J.*, **35**(4), 599-609. https://doi.org/10.12989/scs.2020.35.4.599.

Shariati, M., Ramli Sulong, N.H. and Arabnejad Khanouki, M.M. (2012a), "Experimental assessment of channel shear connectors under monotonic and fully reversed cyclic loading in high strength concrete", *Mater. Des.*, **34**, 325-331. https://doi.org/10.1016/j.matdes.2011.08.008.

Shariati, M., Ramli Sulong, N.H., Suhatril, M., Shariati, A., Arabnejad Khanouki, M.M. and Sinaei, H. (2012b), "Behaviour of C-shaped angle shear connectors under monotonic and fully reversed cyclic loading: An experimental study", *Mater. Des.*, **41**, 67-73. https://doi.org/10.1016/j.matdes.2012.04.039.

Shariati, M., Ramli Sulong, N.H., Suhatril, M., Shariati, A., Arabnejad Khanouki, M.M. and Sinaei, H. (2013), "Comparison of behaviour between channel and angle shear connectors under monotonic and fully reversed cyclic loading", *Constr. Build. Mater.*, **38**, 582-593. https://doi.org/10.1016/j.conbuildmat.2012.07.050.

Shariati, M., Toghroli, A., Jalali, A. and Ibrahim, Z. (2017), "Assessment of stiffened angle shear connector under monotonic and fully reversed cyclic loading", *Proceedings of the Fifth International Conference on Advances in Civil, Structural and Mechanical Engineering-CSM 2017*, Bangkok, Thailand, September.

Shariati, M., Tahir, M.M., Wee, T.C., Shah, S., Jalali, A., Abdullahi, M.A.M. and Khorami, M. (2018), "Experimental investigations on monotonic and cyclic behavior of steel pallet rack connections", *Eng. Fail. Anal.*, **85**, 149-166. https://doi.org/10.1016/j.engfailanal.2017.08.014.

Shariati, M., Azar, S.M., Arjomand, M.A., Tehrani, H.S., Daei, M. and Safa, M. (2019a), "Comparison of dynamic behavior of shallow foundations based on pile and geosynthetic materials in fine-grained clayey soils", *Geomech. Eng.*, *Int. J.*, **19**(6), 473-484. https://doi.org/10.12989/gae.2019.19.6.473.

Shariati, M., Faegh, S.S., Mehrabi, P., Bahavarnia, S., Zandi, Y., Masoom, D.R., Toghroli, A., Trung, N.T. and Salih, M.N. (2019b), "Numerical study on the structural performance of corrugated low yield point steel plate shear walls with circular openings", *Steel Compos. Struct.*, *Int. J.*, **33**(4), 569-581. https://doi.org/10.12989/scs.2019.33.4.569.

Shariati, M., Mafipour, M.S., Mehrabi, P., Bahadori, A., Zandi, Y., Salih, M.N., Nguyen, H., Dou, J., Song, X. and Poi-Ngian, S. (2019c), "Application of a hybrid artificial neural network-particle swarm optimization (ANN-PSO) model in behavior prediction of channel shear connectors embedded in normal and high-strength concrete", *Appl. Sci.*, **9**(24), 5534. https://doi.org/10.3390/app9245534.

Shariati, M., Mafipour, M.S., Mehrabi, P., Zandi, Y., Dehghani, D., Bahadori, A., Shariati, A., Trung, N.T., Salih, M.N. and Poi-Ngian, S. (2019d), "Application of extreme learning machine (ELM) and genetic programming (GP) to design steel-concrete composite floor systems at elevated temperatures", *Steel Compos. Struct.*, *Int. J.*, **33**(3), 319-332. https://doi.org/10.12989/scs.2019.33.3.319.

Shariati, M., Trung, N.T., Wakil, K., Mehrabi, P., Safa, M. and Khorami, M. (2019e), "Moment-rotation estimation of steel rack connection using extreme learning machine", *Steel Compos. Struct.*, *Int. J.*, **31**(5), 427-435. https://doi.org/10.12989/scs.2019.31.5.427.

Shariati, M., Azar, S.M., Arjomand, M.A., Tehrani, H.S., Daei, M. and Safa, M. (2020a), "Evaluating the impacts of using piles and geosynthetics in reducing the settlement of fine-grained soils under static load", *Geomech. Eng.*, *Int. J.*, **20**(2), 87-101. https://doi.org/10.12989/gae.2020.20.2.087.

Shariati, M., Mafipour, M.S., Ghahremani, B., Azarhomayun, F., Ahmadi, M., Trung, N.T. and Shariati, A. (2020b), "A novel hybrid extreme learning machine-grey wolf optimizer (ELM-GWO) model to predict compressive strength of concrete with partial replacements for cement", *Eng. Comput.*, **2020**, 1-23. https://doi.org/10.1007/s00366-020-01081-0.

Shariati, M., Mafipour, M.S., Haido, J.H., Yousif, S.T., Toghroli, A., Trung, N.T. and Shariati, A. (2020c), "Identification of the most influencing parameters on the properties of corroded concrete beams using an adaptive neuro-fuzzy inference system (ANFIS)", *Steel Compos. Struct.*, *Int. J.*, **34**(1), 155-170. https://doi.org/10.12989/scs.2020.34.1.155.

Shariati, M., Mafipour, M.S., Mehrabi, P., Ahmadi, M., Wakil, K., Trung, N.T. and Toghroli, A. (2020d), "Prediction of concrete strength in presence of furnace slag and fly ash using hybrid ANN-GA (artificial neural network-genetic algorithm)", *Smart Struct. Syst.*, *Int. J.*, **25**(2), 183-195. https://doi.org/10.12989/sss.2020.25.2.183.

Shariati, M., Mafipour, M.S., Mehrabi, P., Shariati, A., Toghroli, A., Trung, N.T. and Salih, M.N.A. (2020e), "A novel approach to predict shear strength of tilted angle connectors using artificial intelligence techniques", *Eng. Comput.*, **2020**, 1-21. https://doi.org/10.1007/s00366-019-00930-x.

Shariati, M., Naghipour, M., Yousofizinsaz, G., Toghroli, A. and Tabarestani, N.P. (2020f), "Numerical study on the axial compressive behavior of built-up CFT columns considering different welding lines", *Steel Compos. Struct.*, *Int. J.*, **34**(3), 377-391. https://doi.org/10.12989/scs.2020.34.3.377.

Shariati, M., Shariati, A., Trung, N.T., Shoaei, P., Ameri, F., Bahrami, N. and Zamanabadi, S.N. (2020g), "Alkali-activated slag (AAS) paste: Correlation between durability and microstructural characteristics", *Constr. Build. Mater.*, **2020**, 120886 https://doi.org/10.1016/j.conbuildmat.2020.120886.

Shariati, M., Tahmasbi, F., Mehrabi, P., Bahadori, A. and Toghroli, A. (2020h), "Monotonic behavior of C and L shaped angle shear connectors within steel-concrete composite beams: An experimental investigation", *Steel Compos. Struct.*, *Int. J.*, **35**(2), 237-247. https://doi.org/10.12989/scs.2020.35.2.237.

Sinaei, H., Shariati, M., Abna, A.H., Aghaei, M. and Shariati, A. (2012), "Evaluation of reinforced concrete beam behaviour using finite element analysis by ABAQUS", *Sci. Res. Essays*, **7**(21), 2002-2009. https://doi.org/10.5897/SRE11.1393.

Soliman, M.M. (2010), *Engineering Hydrology of Arid and Semi-arid Regions*, CRC Press, New York, USA.

Strand, R. and Pemberton, E. (1987), "Design of small dams",

United States Department of the Interior, Bureau of Reclamation, USA.

Suhatril, M., Osman, N., Sari, P.A., Shariati, M. and Marto, A. (2019), "Significance of surface eco-protection techniques for cohesive soils slope in Selangor, Malaysia", *Geotech. Geol. Eng.*, **37**(3), 2007-2014. https://doi.org/10.1007/s10706-018-0740-3.

Toghroli, A. (2015), "Applications of the ANFIS and LR models in the prediction of shear connection in composite beams", MS.c. Dissertation, University of Malaya, Malaya, Malaysia.

Toghroli, A., Mohammadhassani, M., Suhatril, M., Shariati, M. and Ibrahim, Z. (2014), "Prediction of shear capacity of channel shear connectors using the ANFIS model", *Steel Compos. Struct.*, *Int. J.*, **17**(5), 623-639. http://dx.doi.org/10.12989/scs.2014.17.5.623.

Toghroli, A., Suhatril, M., Ibrahim, Z., Safa, M., Shariati, M. and Shamshirband, S. (2016), "Potential of soft computing approach for evaluating the factors affecting the capacity of steel-concrete composite beam", *J. Intell. Manuf.*, **2016**, 1-9. http://dx.doi.org/10.1007/s10845-016-1217-y.

Toghroli, A., Darvishmoghaddam, E., Zandi, Y., Parvan, M., Safa, M., Abdullahi, M.A.M., Heydari, A., Wakil, K., Gebreel, S.A. and Khorami, M. (2018), "Evaluation of the parameters affecting the Schmidt rebound hammer reading using ANFIS method", *Comput. Concrete*, *Int. J.*, **21**(5), 525-530. https://doi.org/10.12989/cac.2018.21.5.525.

Trung, N.T., Shahgoli, A.F., Zandi, Y., Shariati, M., Wakil, K., Safa, M. and Khorami, M. (2019), "Moment-rotation prediction of precast beam-to-column connections using extreme learning machine", *Struct. Eng. Mech.*, *Int. J.*, **70**(5), 639-647. https://doi.org/10.12989/sem.2019.70.5.639.

Xu, C., Zhang, X., Haido, J.H., Mehrabi, P., Shariati, A., Mohamad, E.T., Nguyen, H. and Wakil, K. (2019), "Using genetic algorithms method for the paramount design of reinforced concrete structures", *Struct. Eng. Mech.*, *Int. J.*, **71**(5), 503-513. https://doi.org/10.12989/sem.2019.71.5.503.

Yang, C.T. (1996), *Sediment Transport: Theory and Practice*, Mcgraw-Hill, New York, USA.

Yazdani, M., Kabirifar, K., Frimpong, B.E., Shariati, M., Mirmozaffari, M. and Boskabadi, A. (2020), "Improving construction and demolition waste collection service in an urban area using a simheuristic approach: A case study in Sydney, Australia", *J. Clean. Prod.*, **2020**, 124138. https://doi.org/10.1016/j.jclepro.2020.124138.

Zabaleta, A., Martínez, M., Uriarte, J.A. and Antigüedad, I. (2007), "Factors controlling suspended sediment yield during runoff events in small headwater catchments of the Basque country", *Catena*, **71**(1), 179-190. https://doi.org/10.1016/j.catena.2006.06.007.

Zandi, Y., Shariati, M., Marto, A., Wei, X., Karaca, Z., Dao, D., Toghroli, A., Hashemi, M.H., Sedghi, Y. and Wakil, K. (2018), "Computational investigation of the comparative analysis of cylindrical barns subjected to earthquake", *Steel Compos. Struct.*, *Int. J.*, **28**(4), 439-447. https://doi.org/10.12989/scs.2018.28.4.439.

Zhao, X., Fourie, A. and Qi, C.C. (2019), "An analytical solution for evaluating the safety of an exposed face in a paste backfill stope incorporating the arching phenomenon", *Int. J. Miner. Metall. Mater.*, **26**(10), 1206-1216. https://doi.org/10.1007/s12613-019-1885-7.

Zhao, X., Fourie, A. and Qi, C.C. (2020a), "Mechanics and safety issues in tailing-based backfill: A review", *Int. J. Miner. Metall. Mater.*, **27**(9), 1165-1178. https://doi.org/10.1007/s12613-020-2004-5.

Zhao, X., Fourie, A., Veenstra, R. and Qi, C.C. (2020b), "Safety of barricades in cemented paste-backfilled stopes", *Int. J. Miner. Metall. Mater.*, **27**(8), 1054-1064. https://doi.org/10.1007/s12613-020-2006-3.

CC